A Comparative Study of Online Impedance Measurement Techniques for a Lithium Polymer Battery

Amrit Sethi[1] and Dries Verstraete[1]

[1]*School of Aerospace, Mechanical and Mechatronic Engineering*
The University of Sydney, Sydney, NSW 2006, Australia

Abstract

As batteries are increasingly used in automotive and aerospace applications, the need to monitor their health and perform diagnostics increases. Among the different batteries, Lithium Polymer (Li-Po) batteries are attractive options due to their high energy, power density, and long life. The degradation factors, state of charge and state of health of batteries are parameters indicative of the battery performance and a sound knowledge of these factors can help improve their efficiency and endurance. These factors can be determined through the impedance of the battery. This paper explores different methods for determining the impedance and compares them in terms of their accuracy and the feasibility of implementing them in an online system.

Keywords: Li-Po battery, impedance, online measurement, Electrochemical Impedance Spectroscopy (EIS), Fast EIS, Equivalent Circuit Modelling (ECM), health diagnostics

1 Introduction

Batteries are increasingly used in electric vehicles [1, 2] and other applications [3] in response to diminishing supplies of fossil fuels as well as to mitigate CO_2 emissions. Among the different batteries, Lithium-Ion (Li-Ion) batteries are attractive options due to their high energy and power density and long life[4] and have found their use in various applications [5]. Li-Po batteries differ as they contain a metallic anode and a solid polymer for the electrolyte [6]. With increasing use, the need to improve their performance becomes more apparent. Li-Po battery performance can be improved by understanding their electrochemical processes and obtaining the impedance of a battery in real time.

1.1 Impedance of a Battery

The battery uses Lithium ions in galvanic reactions to convert chemical energy to electrical energy and vice-versa [7] and comprises of the anode (the negative electrode), the cathode (the positive electrode), and the electrolyte that allows ion transport between the electrodes. To separate the electrodes electrically and mechanically, an inert separator is placed between the electrodes. The losses associated with the reactions occurring in a battery are as follows [7–9]:

- Ohmic Losses - this is caused by the resistance associated with the different battery components. It should be noted that the resistance associated with the contact surfaces in a battery is incorporated into the ohmic losses for simplification [9]. The losses are prominent at high frequencies.
- Activation Losses - These are the losses associated with the activation barrier of the chemical reactions involved. This includes charge transfer reactions and self-discharge of the battery
- Concentration Losses - These are the losses associated with the variations in reactant concentrations across the cell. This includes losses associated with the diffusion of reactants.

1.2 Finding the Impedance

Various dynamic processes of a Li-Po battery can be examined through its impedance. This impedance can be obtained in several different ways by examining the current-voltage characteristics of the battery. These characteristics can be determined by various methods, such as Electrochemical Impedance Spectroscopy (EIS), Fast/Square EIS and curve fitting. While they differ in their implementation, they all involve applying a changing an electrical condition (such as current or voltage), measuring the resulting waveforms and estimating parameters to model this change [10]. This study examines the use of EIS, Fast EIS, optimisation of current-voltage data and state estimation as tools for deriving the impedance in an online setting in terms of absolute and relative accuracy, as well as computation time and feasibility in an online context.

1.2.1 Electrochemical Impedance Spectroscopy

Electrochemical Impedance Spectroscopy (EIS) [10] is a technique in which an AC perturbation at a particular frequency is applied to a DC signal. The impedance at that frequency is then derived from the resulting changes in magnitude and phase. To enable a detailed examination, this process is repeated over a range of frequencies and is usually displayed on a Nyquist plot.

Examination of a multitude of frequencies reveals the various electrochemical phenomena that characterize the battery behaviour. Due to this, EIS has been used extensively in literature [11, 12] and is used as the benchmark to which other tests are compared.

1.2.2 Fast EIS

Numerous methods use the frequency content and magnitude of the current-voltage data in response to a short-term perturbation in order to determine the impedance [13]. The various methods differ in the manner in which they transfer the data to the frequency domain and in the signal they use. Three methods are primarily used for transforming the time data to the frequency domain [13] - Fourier Transform, Laplace Transform, and Wavelet Transform. To retrieve maximal information through the different transforms, the signal used is often rich in frequency content. This includes white noise, multi-sine waves, chirp signals, and pseudo-random signals [13, 14]. This study specifically adapts the method from refs. [15, 16], also known as Fast EIS, due to its sophistication without requiring significant equipment. The method employs a probabilistic model and uses the wavelet transform results of a pseudo-random signal (PRBS) to accurately determine the impedance of the system being tested at various frequencies. In essence, the impedance is determined by finding the ratio of the complex wavelet coefficients associated with the voltage and current data. PRBS can cover a band of frequencies with the -3dB cut-off point corresponding to a third of the sampling frequency.

1.3 Curve fitting

An equivalent circuit model (ECM) is often used to model the battery dynamics [17, 18]. These circuits vary in complexity and to employ the ECM for useful analysis, the values of the circuit elements need to be found. To encapsulate general battery dynamics with minimal complexity, the ECM shown in Figure 1 is used [19].

The voltage-current characteristics from this circuit model for single step can be represented in time using Equation 1 [19]:

$$\begin{aligned} V = V_{OC} - i_L R_0 - U_{PA0} exp\left(\frac{-t}{R_{PA}C_{PA}}\right) - U_{PC0} exp\left(\frac{-t}{R_{PC}C_{PC}}\right) \\ - R_{PA} i_L \left[1 - exp\left(\frac{-t}{R_{PA}C_{PA}}\right)\right] - R_{PC} i_L \left[1 - exp\left(\frac{-t}{R_{PC}C_{PC}}\right)\right] \end{aligned} \tag{1}$$

This equation represents the activation and concentration losses. In our study, we use a step over 0.5s extracted from the PRBS signal used by the Fast EIS to obtain the parameters. Curve fitting using Levenberg–Marquardt was employed to determine the parameters.

This study looks at EIS, Fast EIS and curve fitting using the ECM to determine the battery impedance. The results at various states of charge (SOC) are used to see the differences across the full operation of the battery. The experimental set-up involved is first explained and then these methods are compared in terms of accuracy and suitability to be applied in an online context.

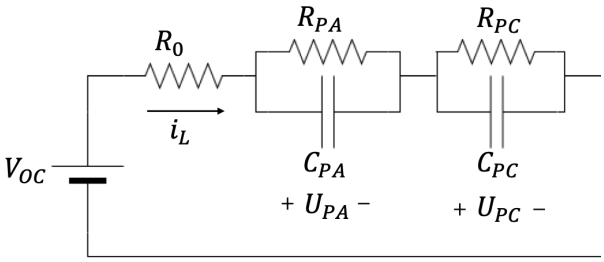

Figure 1: The Equivalent Circuit Model Used

2 Experimental Set-Up

A 4 cell 1000mAh Turnigy Graphene lithium-ion battery is used for the tests. Impedance measurements are made with the Biologic SP-300 frequency response analyser (FRA) connected to the HCV-3048 and HC-10 current and voltage boosters. With this combination, impedance measurements from 500 kHz to 10 μHz can be achieved. Current accuracy is 0.1% $\pm$ 0.3% (percentages correspond to the full scale and reading respectively) for the 0 to 30A range while the voltage measurements have an accuracy

of 0.03% $\pm$ 0.03% in the range of 0 to 48V. The battery is charged to 100% state of charge and slowly discharged at 2C until the state of charge reaches a multiple of 10% between 20% and 90%. Subsequently, 3 PRBS signals are applied in succession with sampling frequencies of 100Hz, 10Hz and 2Hz for 2,6 and 2 seconds respectively. This is followed by the EIS measurement.

3 Results

The impedances obtained using the three methods are shown in Figures 2a, 2b and 2c. To allow for comparisons, Figure 3 contains the figures comparing the three methods directly at specific states of charge.

Figures 2a, 2b and 2c have specific common features. The most prominent feature is the increase in arc length with decreasing states of charge. The arc length, based on literature, can be directly correlated with the charge transfer resistance. This value, in turn, denotes the ease with which the charge transfer process is facilitated. The dependency of the charge transfer resistance varies with cell chemistry as while some studies show strong relations [9, 12], others show little to no variation [20]. Ref. [12] delves into this aspect in more detail but essentially, it can be explained by the uneven distribution of charges at higher depths of discharge. Although lower frequencies are not examined in this study, the diffusion losses would also show significant differences and seem to affect the points associated with low frequencies in Figure 2b. Based on theory, diffusion losses are expected to be prominent [7] because low states of charge imply that the concentration of Li-ions is uneven throughout the cell. Since the diffusion due to the concentration gradient counteracts the usual flow of ions in the discharge process, higher losses occur at lower states of charge.

The impedance associated with the highest frequencies seem to vary slightly with SOC. This seems to be in accordance with literature [18] which show slight non-linear relations.

3.1 Comparing the methods

Impedances derived at specific states of charge are used to compare the accuracy of the different methods. These are shown in Figure 3. The most notable aspect of the comparisons is the high similarities between the EIS and Fast EIS values. The Fast EIS values seem to closely follow the actual EIS values in most cases. However, it seems like there are diversions between the two datasets at higher frequencies. This could be attributed to the range of frequencies that we are capable of observing using the PRBS signals. Furthermore, the Fast EIS method operates on probability distribution and each impedance point is a part of a distribution for a particular frequency. Although this was factored in when selecting the optimal impedance point, it is possible that points with a lower probability were perhaps more accurate for low frequency values. The general trends between the EIS and Fast EIS results, as seen in Figures 2a and 2b, remain the same. For most purposes, therefore, Fast EIS seems to be a suitable alternative to EIS for online measurements.

The circuit modelling approach, though, lead to significant differences between the actual impedance values and derived impedance values. The fit, however, appears to better at higher states of charge. This could be because more complex losses come into play at lower states of charge resulting in dynamics that the ECM is unable to capture. It appears that the impedance obtained through curve-fitting are good for understanding trends but are not suitable for making direct comparisons with the EIS and Fast EIS results. The most obvious proponent of this hypothesis is the increasing arc lengths in Figure 2c - suggesting that the charge transfer resistance increases with increasing depth of discharge. This is in line with theory as well as the EIS and Fast EIS results. The ECM derived impedances also seem to suggest a stronger trend between the state of charge and $R0$ than obtained through EIS and Fast EIS results. Equivalent circuit models have found widespread use in system identification and state estimation when trying to better understand battery characteristics [18, 19]. The curve fitting process only looks at the current-voltage data in the time domain when trying to find parameters using Equation 1 and does not consider the frequency content separately. While this approach allows for good fits and helps differentiate the battery parameters in relative terms, it is not suitable for direct comparisons with EIS or Fast EIS data for impedance measurement.

3.2 Suitability for online measurements

The use of the methods in an online context varies in terms of the equipment required as well as computation times. On Matlab, the curve fitting took 0.408s while Fast EIS took 2.180s. These were on a Windows 10 PC with 8GB of RAM and an i7 processor with 3.40GHz processor speed. The Fast EIS method requires the use of the wavelet transform and calculations involving complex number which increase the computation time required. The wavelet transform calculations alone took 1.5s. The wavelet process can be run in parallel if multiple cores are present in the processor [21], to make it more suitable for real-time operation. However, this would increase expenses. In ref. [16], a portable

system was designed that would perform the process in real-time. On the other hand, the optimisation problem is more straightforward to implement, requires only a single step in terms of data. However, it cannot be run in parallel and it does not have a fixed computation time associated with it - potentially making it unreliable if the initial parameters are significantly more different than the actual parameters. When compared to the Fast EIS method though, the curve fitting method provides parameter values associated with the ECM which may be used for analysis directly without computing the impedance. It should be noted that an IC has been developed for applying EIS to batteries but would still require a sine wave with varying frequencies [22].

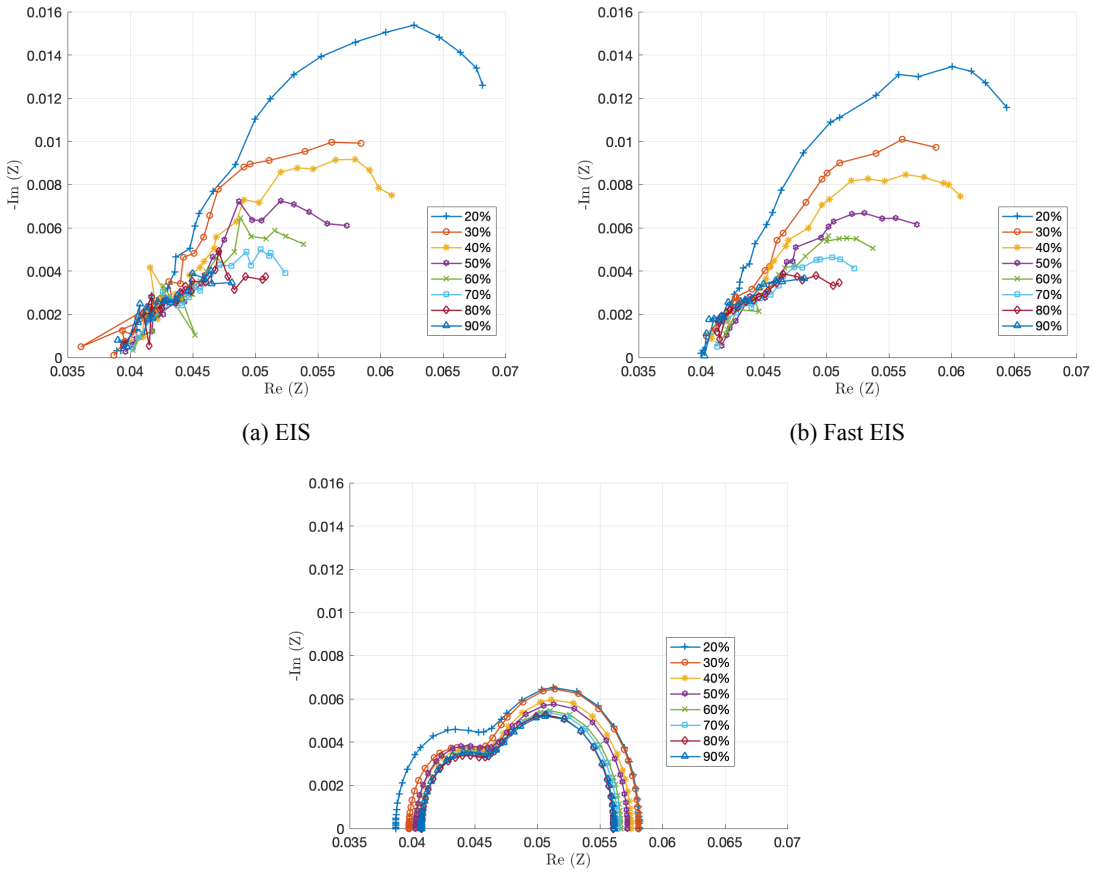

(a) EIS

(b) Fast EIS

(c) Curve Fitting

Figure 2: Impedances derived using different methods

4 Conclusion

This study looks at Fast EIS and the use of optimisation to fit data to an ECM and compares them in terms of accuracy (when compared to the actual EIS results) and suitability in an online context. It should be noted that the study assesses the online suitability of the different methods by applying them offline. Fast EIS provided high accuracy but at the cost of high computation times. On the other hand, curve fitting provided lower accuracy at a much faster rate. It also used a single step of data instead of the full PRBS signal. The trends obtained through curve fitting also allow for discrimination of SOCs. The fast computation times, though, are highly dependent on the initial guess. Fast EIS is relatively fixed computationally regardless of the data. The algorithm for curve fitting is simpler and thus more cost effective as it requires less computational complexity. Choosing a suitable method for health diagnostics depends on the values that are needed, the accuracy of those values and the computation as there is a clear tradeoff involved. Future studies could examine the sensitivity of the various methods to measurement errors and lower sampling rates.

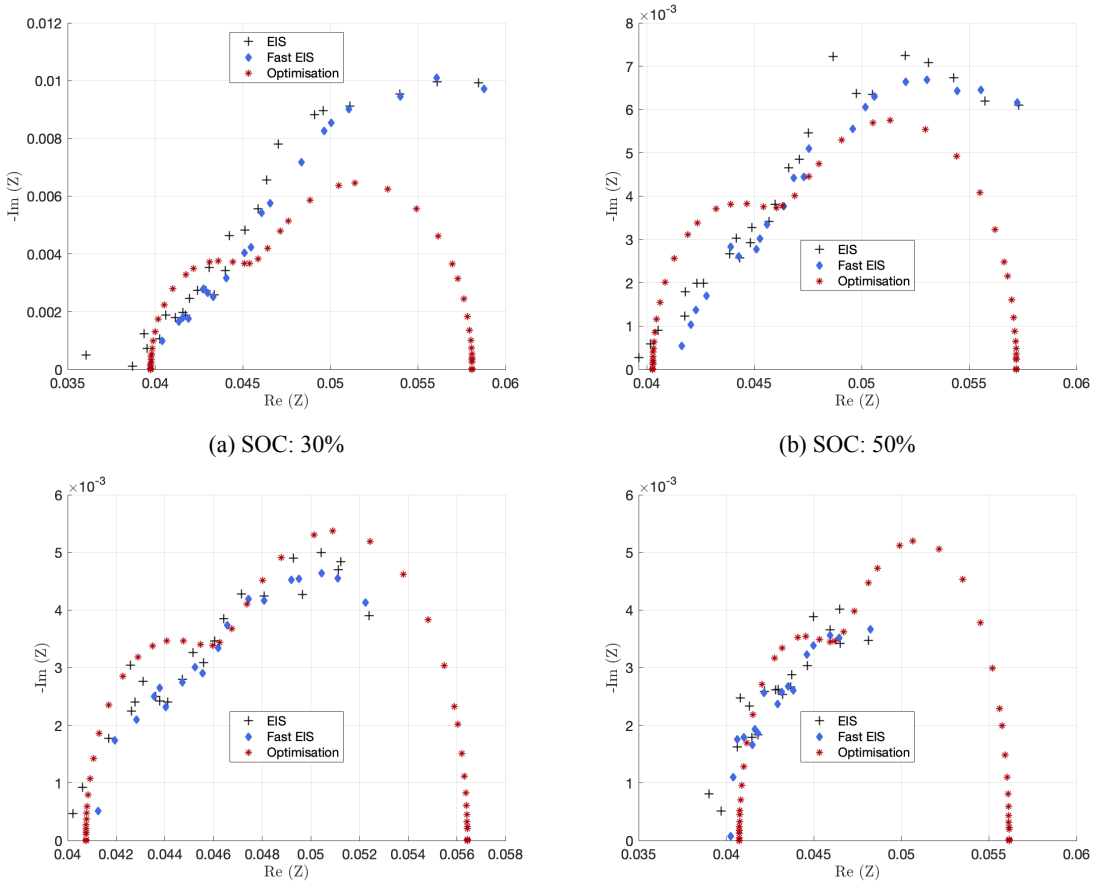

(a) SOC: 30%

(b) SOC: 50%

(c) SOC: 70%

(d) SOC: 90%

Figure 3: The results from the various methods at specific States of Charge

5 Bibliography

[1] M.S. Hossain Lipu, M.A. Hannan, Aini Hussain, M.M. Hoque, Pin J. Ker, M.H.M. Saad, and Afida Ayob. A review of state of health and remaining useful life estimation methods for lithium-ion battery in electric vehicles: Challenges and recommendations. *Journal of Cleaner Production*, 205:115–133, 2018.

[2] Siang Fui Tie and Chee Wei Tan. A review of energy sources and energy management system in electric vehicles. *Renewable and Sustainable Energy Reviews*, 20:82–102, 2013.

[3] C.M. Reid, M.A. Manzo, and M.J. Logan. Performance characterization of a lithium-ion gel polymer battery power supply system for an unmanned aerial vehicle. *NASA TM2004-213401*, 2004.

[4] Languang Lu, Xuebing Han, Jianqiu Li, Jianfeng Hua, and Minggao Ouyang. A review on the key issues for lithium-ion battery management in electric vehicles. *Journal of Power Sources*, 226:272–288, 2013.

[5] Dries Verstraete, Andrew Gong, Dylan D C Lu, and Jennifer L. Palmer. Experimental investigation of the role of the battery in the AeroStack hybrid, fuel-cell-based propulsion system for small unmanned aircraft systems. *International Journal of Hydrogen Energy*, 40(3):1598–1606, 2015.

[6] K.T. Chau, Y.S. Wong, and C.C. Chan. Overview of energy sources for electric vehicles. *Energy Conversion and Management*, 40(10):1021–1039, 1999.

[7] Bhaskar Saha, Patrick Quach, and Kai Goebel. Exploring the model design space for battery health management. *Prognostics and Health Management*, (January):1–8, 2011.

[8] Bhaskar Saha, Cuong C. Quach, and Kai Goebel. Optimizing battery life for electric UAVs using a Bayesian framework. *IEEE Aerospace Conference Proceedings*, pages 1–7, 2012.

[9] Sophia Gantenbein, Michael Weiss, and Ellen Ivers-Tiffée. Impedance based time-domain modeling of lithium-ion batteries: Part I. *Journal of Power Sources*, 379(September 2017):317–327, 2018.

[10] K. R. Cooper and M. Smith. Electrical test methods for on-line fuel cell ohmic resistance measurement. *Journal of Power Sources*, 160(2 SPEC. ISS.):1088–1095, 2006.

[11] M.A. Hannan, M.S.H. Lipu, A. Hussain, and A. Mohamed. A review of lithium-ion battery state of charge estimation and management system in electric vehicle applications: Challenges and recommendations. *Renewable and Sustainable Energy Reviews*, 78(August 2016):834–854, 2017.

[12] M. Schönleber, C. Uhlmann, P. Braun, A. Weber, and E. Ivers-Tiffée. A Consistent Derivation of the Impedance of a Lithium-Ion Battery Electrode and its Dependency on the State-of-Charge. *Electrochimica Acta*, 243:250–259, 2017.

[13] Tokihiko Yokoshima, Daikichi Mukoyama, Hiroki Nara, Suguru Maeda, Kazuhiro Nakazawa, Toshiyuki Momma, and Tetsuya Osaka. Impedance Measurements of Kilowatt-Class Lithium Ion Battery Modules/Cubicles in Energy Storage Systems by Square-Current Electrochemical Impedance Spectroscopy. *Electrochimica Acta*, 246:800–811, 2017.

[14] Brian Bullecks, Resmi Suresh, and Raghunathan Rengaswamy. Rapid impedance measurement using chirp signals for electrochemical system analysis. *Computers and Chemical Engineering*, 106(June 2017):421–436, 2017.

[15] Andrej Debenjak, Pavle Boškoski, Bojan Musizza, Janko Petrovčič, and Crossed D.Signani Juričić. Fast measurement of proton exchange membrane fuel cell impedance based on pseudo-random binary sequence perturbation signals and continuous wavelet transform. *Journal of Power Sources*, 254:112–118, 2014.

[16] P. Boškoski, A. Debenjak, and B. Mileva Boshkoska. Hardware components for condition monitoring of pem fuel cells. *SpringerBriefs in Applied Sciences and Technology*, pages 65–77, 2017.

[17] Bizhong Xia, Zhen Sun, Ruifeng Zhang, Deyu Cui, Zizhou Lao, Wei Wang, Wei Sun, Yongzhi Lai, and Mingwang Wang. A comparative study of three improved algorithms based on particle filter algorithms in SOC estimation of lithium ion batteries. *Energies*, 10(8):1–14, 2017.

[18] Yasser Diab, François Auger, Emmanuel Schaeffer, and Moutassem Wahbeh. Estimating Lithium-Ion Battery State of Charge and Parameters Using a Continuous-Discrete Extended Kalman Filter. *Energies*, 10(8), 2017.

[19] Zhihao Yu, Ruituo Huai, and Linjing Xiao. State-of-charge estimation for lithium-ion batteries using a Kalman filter based on local linearization. *Energies*, 8(8):7854–7873, 2015.

[20] Haifeng Dai, Bo Jiang, and Xuezhe Wei. Impedance Characterization and Modeling of Lithium-Ion Batteries Considering the Internal Temperature Gradient. *Energies*, 11(1):220, 2018.

[21] Bharatkumar Sharma and Naga Vydyanathan. Parallel discrete wavelet transform using the open computing language: A performance and portability study. *Proceedings of the 2010 IEEE International Symposium on Parallel and Distributed Processing, Workshops and Phd Forum, IPDPSW 2010*, 2010.

[22] Z. Gong, Z. Liu, Y. Wang, K. Gupta, C. Da Silva, T. Liu, Z. H. Zheng, W. P. Zhang, J. P.M. Van Lammeren, H. J. Bergveld, C. H. Amon, and O. Trescases. IC for online EIS in automotive batteries and hybrid architecture for high-current perturbation in low-impedance cells. *Conference Proceedings - IEEE Applied Power Electronics Conference and Exposition - APEC*, 2018-March:1922–1929, 2018.